

Supporting Information for "Relevance of dissolved organic nutrients for the Arctic Ocean nutrient budget"

Sinhué Torres-Valdés,¹ Takamasa Tsubouchi,^{2,3} Emily Davey,⁴ Igor Yashayaev,⁵ Sheldon Bacon²

Contents of this file

1. Text S1 to S3
2. Figures S1 to S2
3. Tables S1 to S2

Introduction

This supplementary material contains a more detailed description of sample collection and nutrient analysis (Text S1), a brief description of the method followed to generate mean nutrient profiles (Text S2), and an assessment of uncertainties associated with nutrient transports (Text S3). We also present: (1) additional data to support our description –in the main text– of dissolved inorganic nutrient distributions and contribution of the dissolved organic nutrient pools to the total dissolved nutrient pools (Figure S1); (2) Dis-

Corresponding author: S. Torres-Valdés, Ocean Biogeochemistry and Ecosystems, National Oceanography Centre, European Way, Southampton, SO14 3ZH, UK. (sinhue@noc.ac.uk)

¹Ocean Biogeochemistry and Ecosystems,

15 solved organic nutrients plotted in T-S space; the method we adopted to select DON and
16 DOP concentrations representative of outflowing and inflowing waters from and to the
17 Arctic Ocean.

National Oceanography Centre. European
Way, Southampton, SO14 3ZH, UK.

²Marine Physics and Ocean Climate,
National Oceanography Centre. European
Way, SO14 3ZH, Southampton, UK.

³Now at Physical Oceanography of Polar
Seas, Alfred Wegener Institute for Polar and
Marine Research. Bussestraße 24, D-27570
Bremerhaven, Germany.

⁴Ocean and Earth Science, University of
Southampton, Water Front Campus,
National Oceanography Centre. European
Way, Southampton, SO14 3ZH, UK.

⁵Ocean Sciences Division, Department of
Fisheries and Oceans, Bedford Institute of
Oceanography. PO Box 1006, Dartmouth,
N. S. B2Y 4A2, Canada.

Text S1. Sample Analysis

Samples for nutrient analysis were collected directly into sample-prewashed 60 mL polystyrene vials and stored at -20°C until analysis, <4 months after collection. Dissolved inorganic (nitrate+nitrite and phosphate) and total dissolved nutrients (TDN and TDP) were measured as described in *Torres-Valdés et al.* [2009], using a Seal Analytical QuAA-tro autoanalyser and two 705 Metrohm UV oxidation units. Briefly, frozen samples were defrosted overnight and thoroughly mixed before analysis. Each sample was then split; two 10 mL aliquots were UV-oxidised for 2 h, and a third aliquot was used to measure the dissolved inorganic fraction. Upon UV-oxidation, total dissolved nutrients were measured as nitrate and phosphate. DON and DOP were obtained as the difference between the total and inorganic fractions. Analytical uncertainty associated with the measurement of organic nutrients was estimated as the root-sum-square of total nutrients uncertainty and inorganic nutrient uncertainty. The former derives from duplicate UV-oxidations and the latter from the global uncertainty associated with the analysis of calibration standards (i.e. representative of the duration of the analysis, across all concentrations). Overall, uncertainty was highest at depth, where differences between total and inorganic fractions are small or negligible. Detection limits (DL) were $0.016 \mu\text{mol L}^{-1}$ (phosphate), $0.06 \mu\text{mol L}^{-1}$ (nitrate+nitrite; nitrate hereafter), $0.4 \mu\text{mol L}^{-1}$ (DON) and $0.03 \mu\text{mol L}^{-1}$ (DOP). The average DON and DOP measurement uncertainties for samples from the Nordic Seas were $0.11 \pm 0.08 \mu\text{mol L}^{-1}$ and $0.013 \pm 0.012 \mu\text{mol L}^{-1}$ (respectively), and $0.17 \pm 0.29 \mu\text{mol L}^{-1}$ and $0.08 \pm 0.07 \mu\text{mol L}^{-1}$ (respectively), for samples from the Labrador Current and central and east Labrador Sea.

Text S2. Mean DON and DOP profiles

Following selection of data based on the T-S properties of water masses of interest (as described in the main text), mean DON and DOP profiles were generated for the Labrador Current (LC), East Greenland Current (EGC), West Spitsbergen Current (WSC) and Barents Sea Opening (BSO) inflow as follows. Samples were taken at variable depths, thus, nutrient profiles were generated by linear interpolation at 1 m intervals. Interpolated profiles were then horizontally averaged per water mass to yield mean profiles for outflowing and inflowing waters (Figure 2 main text). That is, only profiles associated the LC, EGC, WSC and BSO (i.e. excluding profiles located in the central part of the Nordic Seas and north of Iceland; black and grey symbols in Figure 1, main text). Horizontal averages were carried out only at depths where two or more data points were available at any given depth. Values flagged as anomalous were not considered.

Text S3. Assessment of uncertainties

Uncertainties associated with nutrient transports were addressed as follows. In order to assess whether results from the simple approach employed here yielded transports that are comparable/consistent with transports calculated with the more thorough approach in *Torres-Valdés et al.* [2013] (TV13 hereafter), we: 1) calculated transports of dissolved inorganic nutrients (nitrate and phosphate) using the data associated with the organic nutrients presented here (i.e. analysed from the same samples); 2) calculated transports of inorganic nutrients using the data presented in TV13, but calculated in the same simple fashion as in the current study of organic nutrients; 3) we compare transports associated with the Labrador Current and/or west Davis Strait and those associated with Bering

Strait, with the full depth integrated transports across west Davis Strait and Bering Strait as calculated in TV13; 4) Finally, transport uncertainties were simply propagated as follows $\sigma^2 = [Vsd(C_n)]^2 + [C_nsd(V)]^2 + 2VC_n\rho sd(V)sd(C_n)$, with volume transport (V) and associated uncertainty $sd(V)$ from *Tsubouchi et al.* [2012], mean nutrient concentration profile (C_n) and associated uncertainty ($sd(C_n)$), and correlation of uncertainties ($\rho sd(V)sd(C_n)$). Given $\rho sd(V)sd(C_n)$ is unknown, we calculated σ^2 assuming no correlation ($\rho = 0$), positive correlation ($\rho = 1$) and inverse correlation ($\rho = -1$).

Table S1 shows volume transports and mean DON and DOP profile concentrations as per Table 1 (main text). It also shows mean nitrate and phosphate profile concentrations from data associated with the DON and DOP, and from the data presented in TV13, but processed in the simple fashion. Remarkably, given the associated uncertainties, mean concentrations are rather consistent between the different data sets. The only exception being nitrate and phosphate concentrations in the EGC, but this is due to the average nutrient profile from *Torres-Valdés et al.* [2013] exhibiting low concentrations deeper in the water column, which it is likely the result of inter-annual variability. Since transports are calculated relative to DON and DOP transports, those calculated for the EGC, WSC and BSO, are focused in the upper 100 m of the water column.

Table S2 shows transports of DON and DOP as per Table 1 (main text), transports of inorganic nutrients associated with the DON and DOP data presented here, transports of inorganic nutrients calculated with data from TV13, and full depth integrated nutrient transports for west Davis Strait and Bering sea as presented in TV13 (see their Table 1). Uncertainties associated with transports calculated the simple way show what we term

‘base uncertainty’ (i.e. no uncertainty correlation) and ‘maximum uncertainty’. With the exception of transports associated with the EGC, which are low due to the mean profile concentration being low further at depth, the remaining transports are remarkably consistent and comparable given both, the base and the maximum estimated uncertainty.

When transports associated with the LC and west Davis Strait (data from TV13) and those for Bering Strait are compared with the full depth integrated transports across west Davis Strait and Bering Strait, again, we can see these are rather consistent within the uncertainty. Bering Strait transports calculated the simple way yield a much larger uncertainty due to the extremely strong horizontal gradients across Bering Strait, with high concentrations of phosphate ($\geq 2.4 \text{ } \mu\text{mol L}^{-1}$) and nitrate ($\geq 24 \text{ } \mu\text{mol L}^{-1}$) on the western side, and low concentrations ($\lesssim 0.7 \text{ } \mu\text{mol-phosphate L}^{-1}$) or undetectable concentrations on the eastern side (see TV13). Indeed, uncertainties calculated the simple way, reflect spatial variability. In TV13, net transports result from vertical and horizontal integration per station pair across gateways, and the uncertainty derives from a thorough sensitivity analysis that considered measured velocity uncertainty and the use of nutrient fields from different years.

That being said, the approach employed here, while simple, yields results which are comparable to the more robust assessment of TV13.

We also assessed what the effect would be in the inferred transports across (west) Davis Strait if; 1) DON from central and east Labrador Sea (off the West Coast of Greenland; Figure 1 main text), and 2) DOP from central Labrador Sea were representative of the northward flowing waters associated with the West Greenland Current. In the case of

106 DON, the transport is estimated to be $+3.8 \pm 0.47 \text{ kmol s}^{-1}$, which would result in a net
 107 southward transport of $-13.9 \pm 2.38 \text{ kmol s}^{-1}$ across Davis Strait, and a net transport of
 108 $-0.86 \pm 3.11 \text{ kmol s}^{-1}$. Thus, given the uncertainty, the DON net transport (i.e. budget) is
 109 either balanced or results in a minor export. However, the large export of DON via Davis
 110 Strait still holds.

111 For DOP, the northward transport is estimated at $0.05 \pm 0.03 \text{ kmol s}^{-1}$, resulting in a
 112 net southward transport across Davis Strait of $-2.77 \pm 0.36 \text{ kmol s}^{-1}$ and a budget of
 113 $-1.69 \pm 0.5 \text{ kmol s}^{-1}$; i.e. the net “indicative” export inferred across Davis Strait and net
 114 pan-Arctic export still hold.

115 However, 1) while a proportion of waters in central Labrador Sea might have a common
 116 origin upstream (e.g., Irminger Basin) relative to waters flowing northwards across east
 117 Davis Strait, we do not know to what extent DON and DOP in upper layers of central
 118 Labrador Sea have been modified (either produced and/or consumed in transit/locally) to
 119 be representative of the northward flowing waters, including the West Greenland Current
 120 (WGC). A proportion of the northward flow is associated with warm Atlantic waters (see
 121 for example *Grist et al.* [2014]) which occur mostly at depths where DON and DOP are
 122 lowest and/or undetectable (in the case of DOP) relative to surface concentrations where
 123 velocities are highest (as shown by *Tsubouchi et al.* [2012]). 2) We only have 1 profile
 124 in east Labrador Sea (off the west Greenland coast), with DON but no DOP data. The
 125 profile is located at 48.48°W , 60.36°N over a shelf break depth of 990 m, and with the
 126 exception of the upper 100 m, its T-S properties are consistent with waters of Atlantic
 127 origin. The upper part (100 m) of the profile does have a colder and fresher component,

suggesting that a fraction is likely composed of West Greenland Coastal waters, but given we lack information about DON and DOP concentrations in Greenland derived runoff and given the profile is far off shore, we are uncertain of how representative this profile might be of the northward flowing waters associated with the WGC. In terms of size, if full depth integrated transports of inorganic nutrients across Davis Strait (TV13) are considered as a reference, we see that the northward transports of phosphate and nitrate are 15-16% relative to the southward transports, though this may not necessary hold true for dissolved organic species. Hence we think that more uncertainty would be introduced if DON and DOP concentrations from central and east Labrador Sea were considered as representative of northward flowing waters. DON and DOP data associated with Greenland runoff and/or coastal water are needed to constrain northward transports.

References

- Grist, J. P., S. A. Josey, L. Boehme, M. P. Meredith, K. L. Laidre, M. P. Heide-Jørgensen, K. M. Kovacs, C. Lydersen, F. J. M. Davidson, G. B. Stenson, M. O. Hammill, R. Marsh, and A. C. Coward, Seasonal variability of the warm Atlantic water layer in the vicinity of the Greenland shelf break, *Geophysical Research Letters*, 41(23), 8530–8537, doi:10.1002/2014GL062051, 2014.
- Holmes, R. M., J. W. McClelland, B. J. Peterson, S. E. Tank, E. Bulygina, T. I. Eglinton, V. V. Gordeev, T. Y. Gurtovaya, P. A. Raymond, D. J. Repeta, R. Staples, R. G. Striegl, A. V. Zhulidov, and S. A. Zimov, Seasonal and Annual Fluxes of Nutrients and Organic Matter from Large Rivers to the Arctic Ocean and Surrounding Seas, *Estuaries and Coasts*, 35(2), 369–382, doi:10.1007/s12237-011-9386-6, 2011.

- 149 Simpson, K. G., J.-E. Tremblay, Y. Gratton, and N. M. Price, An annual study of inorganic
150 and organic nitrogen and phosphorus and silicic acid in the southeastern Beaufort Sea,
151 *Journal of Geophysical Research*, *113*(C7), C07,016, doi:10.1029/2007JC004462, 2008.
- 152 Torres-Valdés, S., V. M. Roussenov, R. Sanders, S. Reynolds, X. Pan, R. Mather, A. Lan-
153 dolfi, G. A. Wolff, E. P. Achterberg, and R. G. Williams, Distribution of dissolved
154 organic nutrients and their effect on export production over the Atlantic Ocean, *Global*
155 *Biogeochemical Cycles*, *23*, GB4019, doi:10.1029/2008GB003389, 2009.
- 156 Torres-Valdés, S., T. Tsubouchi, S. Bacon, A. C. Naveira Garabato, R. Sanders, F. A.
157 McLaughlin, B. Petrie, G. Kattner, K. Azetsu-Scott, and T. E. Whitledge, Export of
158 nutrients from the Arctic Ocean, *Journal of Geophysical Research*, *118*(4), 1625–1644,
159 doi:10.1002/jgrc.20063, 2013.
- 160 Tsubouchi, T., S. Bacon, A. C. Naverira-Garabato, Y. Aksenov, S. W. Laxon,
161 E. Fahrbach, A. Beszczynska-Möller, E. Hansen, C. M. Lee, and R. B. Ingvaldsen, The
162 Arctic Ocean in summer: a quasi-synoptic inverse estimate of boundary fluxes and wa-
163 ter mass transformation, *Journal of Geophysical Research*, doi:10.1029/2011JC007174,
164 2012.

Table 1. Volume transports (Vol_T in Sv; $1 \text{ Sv} = 10^6 \text{ m}^3 \text{ s}^{-1}$) and associated uncertainty (sd), and mean (overbar) profile nutrient concentrations ($\mu\text{mol L}^{-1}$) with associated uncertainty (sd) used to calculate transports (Table 1 main text and Table S2 supplementary material) of dissolved organic nutrients for the Arctic Ocean. To assess transport uncertainty, calculations were also done with the inorganic nutrient data associated with the DON and DOP, and with data taken from *Torres-Valdés et al.* [2013] but processed as described in the current study.

	LC		EGC		WSC		BSO		BS	Rivers
	mean \pm sd		mean \pm sd		mean \pm sd		mean \pm sd		mean \pm sd	
Vol_T	-3.71 \pm 0.37		-0.87 \pm 0.17		0.64 \pm 0.2		1.64 \pm 0.21		1 \pm 0.1	0.07 ^c
\overline{DON}	4.77 \pm 0.41		4.35 \pm 0.25		5.30 \pm 1.57		5.10 \pm 0.90		3.15 \pm 1.51	
\overline{DOP}	0.76 \pm 0.06		0.06 \pm 0.02		0.11 \pm 0.07		0.14 \pm 0.08		0.76 \pm 0.27	
$\overline{NO_3}$	11.73 \pm 0.87		7.20 \pm 0.82		7.92 \pm 2.53		7.19 \pm 1.45		—	
$\overline{PO_4}$	0.94 \pm 0.03		0.77 \pm 0.08		0.62 \pm 0.12		0.51 \pm 0.08		—	
TV13 Data										
$\overline{NO_3}$	9.21 \pm 0.65		3.12 \pm 1.58		8.41 \pm 1.50		6.81 \pm 1.52		11.0 \pm 10.5	
$\overline{PO_4}$	1.12 \pm 0.09		0.47 \pm 0.06		0.61 \pm 0.08		0.53 \pm 0.08		1.46 \pm 0.66	

^aData from [Tsubouchi et al., 2012]. ^bData from Simpson et al. [2008]. ^cData from Hohmes et al. [2011]; total dissolved phosphorus (includes the inorganic and organic fractions); ^dFull depth integrated transport on west Davis Strait (see Table 1 in Torres-Valdés et al. [2013]).

Table 2. Transports (T_n ; kmol s^{-1}) of dissolved organic nutrients and budget (Net) as per Table 1, main text. Transports of inorganic nutrients and full depth cumulative transports are also shown. Polar outflowing waters, Labrador Current (LC), East Greenland Current (EGC), with last row showing west Davis Strait; Atlantic Inflowing waters associated with the West Spitsbergen Current (WSC) and the Barents Sea Opening (BSO); Bering Strait (BS); River discharge (Rivers). The last row in this table shows full integrated transports for west Davis Strait and Bering Strait as per Table 1 in *Torres-Valdés et al.* [2013]. Nutrient transport uncertainties were simply approximated following $\sigma^2 = [Vsd(C_n)]^2 + [C_nsd(V)]^2 + 2VC_n\rho sd(V)sd(C_n)$, with volume transport (V) and associated uncertainty $sd(V)$ from *Tsubouchi et al.* [2012], mean nutrient concentration profile (C_n) and associated uncertainty ($sd(C_n)$), and correlation of uncertainties ($\rho sd(V)sd(C_n)$). Given $\rho sd(V)sd(C_n)$ is unknown, we calculated σ^2 assuming no correlation ($\rho = 0$), positive correlation ($\rho = 1$) and inverse correlation ($\rho = -1$). In this table we show the 'base uncertainty' (i.e., no uncertainty correlation) and 'maximum uncertainty'.

	LC			EGC			WSC			BSO			BS			Rivers			Net		
	T_n	sd_b	sd_m	T_n	sd_b	sd_m	T_n	sd_b	sd_m	T_n	sd_b	sd_m	T_n	sd_b	sd_m	T_n	sd_b	sd_m	T_n	sd_b	sd_m
DON $_{T_n}$	-17.7	2.33	3.90	-3.79	0.77	0.96	3.39	1.46	2.07	8.36	1.83	2.55	3.15	1.54	1.83	1.92			-4.66	3.08	3.92
DOP $_{T_n}$	-2.82	0.36	0.50	-0.05	0.02	0.03	0.07	0.05	0.07	0.23	0.13	0.16	0.76	0.28	0.35	0.07			-1.74	0.50	0.56
NO $_{3T_n}$	-43.5	5.41	7.57	-6.27	1.42	1.94	5.07	2.27	3.21	11.79	2.81	3.88	—								
PO $_{4T_n}$	-3.49	0.37	0.46	-0.67	0.15	0.20	0.40	0.15	0.20	0.84	0.17	0.24	—								
TV13																					
NO $_{3T_n}$	-34.1	4.17	5.82	-2.71	1.47	1.91	5.38	1.94	2.64	11.17	2.87	3.92	10.6	10.6	11.6						
PO $_{4T_n}$	-4.16	0.53	0.75	-0.41	0.10	0.13	0.39	0.13	0.17	0.87	0.17	0.24	0.68	0.68	0.81						
NO $_{3T_n}^a$	-37.7	4.0											9.0	0.8							
PO $_{4T_n}^a$	-4.5	0.5											1.3	0.1							

^aUncertainty from full depth integrated transports (i.e. cumulative transports) on west Davis Strait and across Bering Strait (see Table 1 in *Torres-Valdés et al.* [2013]).

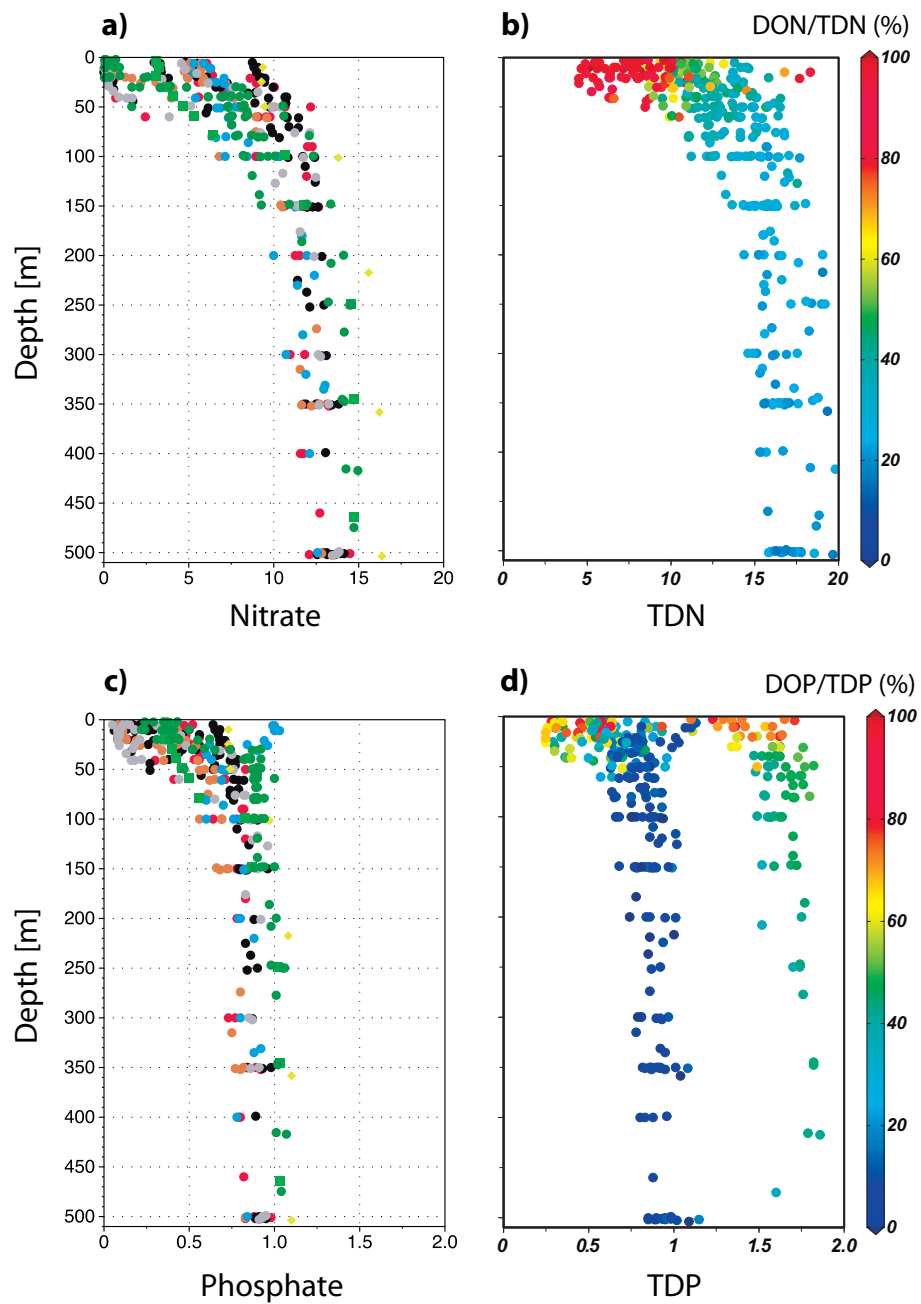


Figure S1. Vertical distribution of nitrate (a), TDN (b), phosphate (c), and TDP (d) in $\mu\text{mol L}^{-1}$. Data points in panels (a), (b), (d) and (e), colour-coded as per Figure 1 (main text). Colour bars in panels (c) and (f) show DON/TDN and DOP/TDP (%).

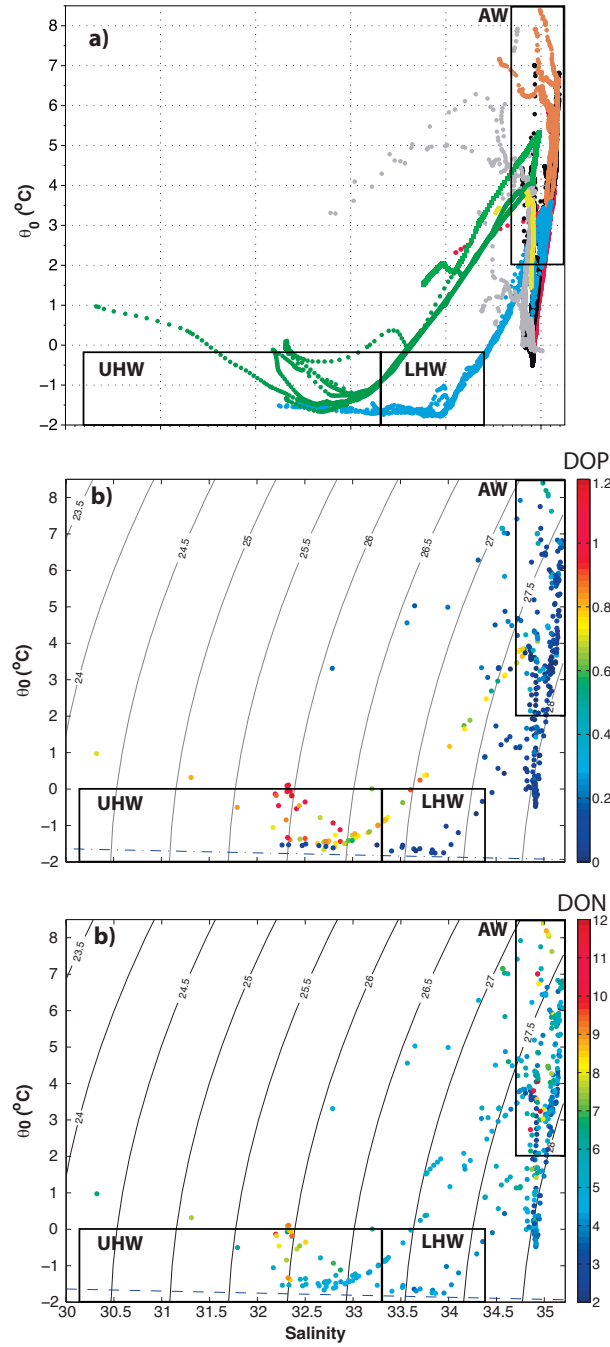


Figure S2. θ_0 -S plots: (a) data colour-coded as per Figure 1 (main text) for reference; DOP (b) and DON (c) plotted on θ_0 -S space. T-S boxes shown for (i) Atlantic Water (AW) and (ii) Polar Waters; Upper Halocline Water (UHW) and Lower Halocline Water (LHW). Blue dashed-dotted line shows the freezing temperature. Colour bar shows nutrient concentration ($\mu\text{mol L}^{-1}$). Following the selection of nutrient concentrations per water mass, station locations were colour-coded as shown in Figure 1.